

## CCN2 as a novel molecule supporting energy metabolism of chondrocytes

Aya Maeda-Uematsu,<sup>1,2</sup> Satoshi Kubota,<sup>1,3</sup> Harumi Kawaki,<sup>1</sup> Kazumi Kawata,<sup>1</sup> Yoshiaki Miyake,<sup>4</sup> Takako Hattori,<sup>1</sup> Takashi Nishida,<sup>1</sup> Norifumi Moritani,<sup>2</sup> Karen M. Lyons,<sup>5</sup> Seiji Iida,<sup>2</sup> and Masaharu Takigawa<sup>1,3</sup>

<sup>1</sup>*Department of Biochemistry and Molecular Dentistry,* <sup>2</sup>*Department of Oral and Maxillofacial Reconstructive Surgery, Okayama University Graduate School of Medicine, Dentistry and Pharmaceutical Sciences;* <sup>3</sup>*Advanced Research Center for Oral and Craniofacial Sciences, Okayama University Dental School;* <sup>4</sup>*Department of Orthopaedic Surgery, Okayama University Graduate School of Medicine, Dentistry and Pharmaceutical Sciences, Okayama, Japan;* <sup>5</sup>*Department of Orthopedic Surgery, UCLA School of Medicine, Los Angeles, CA.*

*Running head: CCN2 as an energy supporter of chondrocytes*

*Keywords: CCN2; CTGF; cartilage; chondrocytes; metabolism*

*Total number of figures: 8*

**Authors for correspondence:** Satoshi Kubota and Masaharu Takigawa

Department of Biochemistry and Molecular Dentistry, Okayama University Graduate School of Medicine, Dentistry and Pharmaceutical Sciences, 2-5-1 Shikata-cho, Okayama 700-8525 Japan

Phone: +81-86-235-6645 FAX: +81-86-235-6649

E-mail: kubota1@md.okayama-u.ac.jp (SK), takigawa@md.okayama-u.ac.jp (MT)

**Contract grant sponsor:** Japan Society for the Promotion of Science

**Contract grant numbers:** #24390415 to M.T. and #25462886 to S.K.

## **Abstract**

CCN2/connective tissue growth factor (CTGF) is a unique molecule that promotes both chondrocytic differentiation and proliferation through its matricellular interaction with a number of extracellular biomolecules. This apparently contradictory functional property of CCN2 suggests its certain role in basic cellular activities such as energy metabolism, which is required for both proliferation and differentiation. Comparative metabolomic analysis of costal chondrocytes isolated from wild-type and *Ccn2*-null mice revealed overall impaired metabolism in the latter. Among the numerous metabolites analyzed, stable reduction in the intracellular level of ATP, GTP, CTP or UTP was observed, indicating a profound role of CCN2 in energy metabolism. Particularly, the cellular level of ATP was decreased by more than 50 % in the *Ccn2*-null chondrocytes. The addition of recombinant CCN2 (rCCN2) to cultured *Ccn2*-null chondrocytes partly redeemed the cellular ATP level attenuated by *Ccn2* deletion. Next, in order to investigate the mechanistic background that mediates the reduction in ATP level in these *Ccn2*-null chondrocytes, we performed transcriptome analysis. As a result, several metabolism-associated genes were found to have been up-regulated or down-regulated in the mutant mice. Up-regulation of a number of ribosomal protein genes was observed upon *Ccn2* deletion, whereas a few genes required for aerobic and anaerobic ATP production were down-regulated in the *Ccn2*-null chondrocytes. Among such genes, reduction in the expression of the enolase 1 gene was of particular note. These findings uncover a novel functional role of CCN2 as a metabolic supporter in the growth-plate chondrocytes, which is required for skeletogenesis in mammals.

## **Introduction**

Endochondral ossification is a critical process that determines the skeletal size of vertebrates (Kubota and Takigawa, 2007, 2011; Takigawa, 2013). This sophisticated process is initiated during the development of long bones, which begin as cartilage anlagen, and remains active until the cessation of body growth. Even after the completion of skeletal growth, endochondral ossification recurs upon bone injury and fracture as a central procedure to regenerate bone defects; and it thus is an indispensable biological process throughout life.

The central player of endochondral ossification is the growth-plate chondrocyte, the cell responsible for the growth of long bones and one that follows a characteristic pathway of differentiation. Chondrocytes differentiate from condensed mesenchyme and begin to produce cartilaginous extracellular matrix (ECM) components, such as type II collagen and aggrecan, to form and support the integrity of the cartilage anlagen. These cells initially remain in a quiescent stage and are designated as resting chondrocytes. Subsequently, these resting chondrocytes begin to proliferate, causing the growth of the anlagen while forming a columnar alignment of themselves. After the proliferative stage, these cells undergo a maturation process. Next, chondrocytes near the bone-cartilage junction in the growth plate differentiate into hypertrophic chondrocytes, which cells induce matrix vesicle-mediated calcification, producing type X collagen and matrix metalloproteinase 13 (MMP-13). This calcifying hypertrophic layer of the growing cartilage is invaded by blood vessels and finally replaced by bone tissue (Kubota and Takigawa, 2007, 2011; Takigawa, 2013).

In general, cell proliferation and differentiation are thought to be biologically incompatible events. Consistent with this notion, a significant number of extracellular

signaling factors that promote either proliferation or differentiation have been reported. For example, fibroblast growth factor 2 (FGF2) (Weksler et al., 1999) promotes the proliferation of growth-plate chondrocytes while inhibiting their differentiation. Contrarily, parathyroid hormone (PTH) evidently enhance chondrocytic differentiation, whereas they exert no significant effect on cell proliferation (Takigawa et al., 1981) . However surprisingly, CCN2 was re-discovered as a factor that could promote both cell proliferation and differentiation and even hypertrophy of chondrocytes throughout the process of endochondral ossification. (Takigawa et al., 2003; Perbal and Takigawa, 2005)

CCN2, also known as connective tissue growth factor (CTGF), is a member of the CCN family of secreted multi-functional proteins (Brigstock et al., 2003; Perbal, 2004; Perbal and Takigawa, 2005; Leask and Abraham, 2006; Jun and Lau, 2011). Previous studies showed that the addition of exogenous CCN2 to cultured chondrocytes promoted the proliferation and enhanced their synthesis of proteoglycans concomitant with elevated expression of chondrocyte-associated genes. These data *in vitro* indicate that CCN2 indeed promotes the proliferation and differentiation of chondrocytes (Nakanishi et al., 1997, 2000; Nishida et al., 2000, 2002). Moreover, in other previous studies *in vivo*, proliferative defect was indicated in chondrocytes in neonatal growth plates of *Ccn2*-null mice (Ivkovic et al., 2003; Kawaki et al., 2008). In the same studies, it was also shown that *Ccn2*-deficient growth-plate cartilage exhibits defects in extracellular matrix formation. These *in vivo* data firmly support the *in vitro* finding that CCN2 is a promoter of cell proliferation and differentiation during endochondral ossification. The mechanism by which CCN2 enhances these apparently incompatible events has remained unclear. However, considering that both of these activities require energy

consumption, it is evident that both cell proliferation and differentiation are supported by and under the control of the metabolic system providing energy. Thus, in this present study we aimed at examining the critical role of CCN2 in the energy metabolism of growth-plate chondrocytes.

## **Materials and Methods**

### ***Histochemical analysis***

The CCN2-KO mice used in this study were previously described (Ivkovic et al., 2003). Hind limbs removed at embryonic day (E) 18.5 or E19.5 were fixed with 4% paraformaldehyde (PFA) in 0.1 M phosphate buffer (pH 7.4) for 24 h. The samples were then decalcified with 10% EDTA for 3–7 days, depending on their age prior to embedment in paraffin. Preparation of thin sections and Alcian blue staining was performed as described previously (Kawaki et al., 2008). Paraffin sections after staining were examined under a Microphoto FXA light microscope equipped with a DXM1200 digital camera (Nikon, Kawasaki, Japan). All animal experiments in this study were conducted according to the Guidelines for Animal Research of Okayama University and were approved by the animal committee.

### ***Cell culture***

Costal chondrocytes were isolated from rib cartilage of *Ccn2*-null mice and wild-type littermates at E18.5 or E19.5, following an established protocol as previously described (Kawaki et al., 2008; Hattori et al., 2010). Briefly, after careful elimination of soft tissues by digestion with 0.05% trypsin for 5 min at 37°C, the cartilage was

digested with 3 mg/ml collagenase A (Roche, Basel, Switzerland) for 1.5h at 37°C to liberate the chondrocytes. These cells were then inoculated into 6-well multiplates containing Dulbecco's modified Eagle's medium (DMEM) supplemented with 10% fetal bovine serum (FBS) and incubated at 37°C under 5% CO<sub>2</sub> in air. The isolated chondrocytes were utilized for experiments within 2 passages in culture. Occasionally, the cells were treated with recombinant human CCN2 (Nakanishi et al., 2000) for the desired time period.

### ***Metabolome analysis***

Extraction of total metabolites from murine chondrocytes was performed by the method recommended by Human Metabolome Technologies (Tsuruoka, Japan). The cells isolated from rib cage cartilage were inoculated into a 6-well multi-plate at a density of  $3.6 \times 10^5$  cells/well and were cultured. At confluence, the cells were washed with 5% mannitol solution (Wako, Osaka, Japan) twice and then were scraped and transferred to a centrifuge tube after the addition of methanol containing 10 µM Internal Standard Solution (Human Metabolome Technologies). They were immediately frozen and stored at -80°C until metabolite extraction could be performed. Prior to the analysis, these samples were mixed with chloroform and ultra pure water and centrifuged at 5,000×g for 5 min at 4°C. For removal of proteins, the sample was centrifugally passed through a filter (5 kDa, MILLIPORE, Billerica, MA). The filtrates were centrifuged and dissolved in 25 µl of ultra pure water. Then cationic and anionic metabolite analysis with a capillary electrophoresis time-of-flight mass spectrometer (CE-TOFMS) was performed (Agilent CE-TOFMS system, Agilent Technologies Japan, Ltd., Tokyo, Japan). Cationic metabolites were analyzed by using

a fused silica capillary (i.d. 50  $\mu\text{m}$  $\times$ 80 cm), with Cation Buffer Solution (Human Metabolome Technologies) as the electrolyte at an injection pressure of 50 mbar for 10 sec, where the applied voltage was 27 kV. Electrospray ionization-mass spectrometry (ESI-MS) was performed in the positive-ion mode. The applied capillary voltage was set at 4,000V and the scan range of the spectrometer was from 50 to 1,000 mass-to-charge ratio ( $m/z$ ). Anionic metabolites were analyzed with Anion Buffer Solution (Human Metabolome Technologies) as the electrolyte at an injection pressure at 50 mbar for 25 sec, with an applied voltage of 30 kV. ESI-MS was performed in the negative-ion mode. The applied capillary voltage was set at 3,500V and the scan range of the spectrometer was from 50 to 1,000  $m/z$ . The peaks detected by CE-TOFMS were processed by using software (MasterHands ver.2.9.0.9, Keio Univ., Tokyo, Japan). In this way,  $m/z$  value, migration time, and peak area level were obtained. The peak area level was converted into a relative area level per cell by the following expression:

$$\text{Relative area level} = \text{objective peak area} / (\text{the area of an internal material} \times \text{cell count})$$

As target materials, 108 substances including amino acids, organic acids, sugar phosphoric acids, and the nucleic acids were analyzed. The concentration of each material was calculated in reference to the concentration of the internal standard material (200  $\mu\text{M}$ ).

### ***RNA extraction and real-time reverse-transcription polymerase chain reaction (RT-PCR) analysis***

Total RNA was extracted and purified by using an RNeasy Mini Kit according to the manufacturer's instructions (Qiagen, Hilden, Germany) and was then reverse-transcribed to cDNA by use of avian myeloblastosis virus reverse transcriptase

with an oligo d(T) as a primer (TaKaRa RNA PCR<sup>TM</sup> Kit Ver.3.0, Takara Shuzo, Tokyo, Japan). Quantitative real-time PCR was carried out by using TOYOBO SYBR Green PCR Master Mix (TOYOBO, Osaka, Japan) with a StepOnePlus<sup>TM</sup> Real-Time PCR Systems (Applied Biosystems, CA). Primers used for the amplification of each cDNA were as follow: 5'- GAC AGA GTG GGA GGC GCT TA -3' (sense) and 5'- CTG AGA ATA GAC ATG GCG AAT TTC -3' (antisense) for murine *Eno1*; 5'- GCG AAT TCC TGC CAG TAG CAT ATG CTT G -3' (sense) and 5'- GGA AGC TTA GAG GAG CGA GCG ACC AAA GG -3' (antisense) for murine and human *r18s*; 5'- GCA GGC TAG AGA AGC AGA GC -3' (sense) and 5'- ATG TCT TCA TGC TGG TGC AG -3' (antisense) for human *CCN2*. Formation of proper amplicons was confirmed by melting curve analysis. Data were standardized against the level of 18s rRNA.

#### ***ATP quantification by bioluminescence assay***

The intracellular ATP level was measured by use of an ATP bioluminescence assay kit (Roche), according to manufacturer's recommendations. Briefly, *Ccn2*-null and WT chondrocytes were initially inoculated at a density of  $3.6\text{-}3.7 \times 10^5$  cells/well into 6-well multiplates. After reaching confluence, the cells were seeded at a density of  $2 \times 10^5$  cells/well into 24-well multiplates and further cultured. At confluence, the chondrocytes were collected and suspended in 100  $\mu$ l of phosphate-buffered saline (PBS). Next, 9 volumes of boiling hot 100 mM Tris-HCl containing 4 mM EDTA (pH7.75) was added to the cell suspension, and the cells were boiled for 2 min and thereafter centrifuged at 1,000 x g for 60 s. Fifty microliters of sample/standard was transferred to each well in a 96-well plate. Then, the luciferase reagent was added to the sample/standard, and the emitted light was measured with a luminometer



(Fluoroskan Ascent FL, Thermo Lab Systems, Franklin, MA).

### ***CCN2 Gene Silencing by an siRNA***

CCN2 siRNA (Silencer<sup>®</sup> select Validated siRNA) and negative control siRNA (Silencer<sup>®</sup> select Negative control siRNA) were purchased from Life Technologies (Carlsbad, CA). Si RNA was delivered into the cells by electroporation using Amaxa<sup>™</sup> Human Chondrocyte Nucleofector<sup>™</sup> kit (Lonza) and Amaxa Nucleofector<sup>®</sup> II (Amaxa Biosystems) according to the manufacturer's instructions. In brief, human chondrocytic cell line HCS-2/8 cells ( $1.0 \times 10^6$ ) were transfected with  $100 \mu\text{M}$  siRNAs in the solution for electroporation (Nucleofector solution and supplement:  $100 \mu\text{l}$ ) using electroporation program U-024. Then the cells in DMEM supplemented with 10% FBS were seeded at a density of  $1.0 \times 10^6$  cells/ well into 6-well plate for RNA extraction and at a density of  $2.0 \times 10^5$  cells/ well into 24-well for ATP bioluminescence assay and were incubated at  $37^\circ\text{C}$  under 5%  $\text{CO}_2$  in the air. After 24 hours, the cells were collected for subsequent analyses.

### ***Microarray analysis***

Comparative transcriptome analysis was performed by using a mouse Panorama Micro Array (Sigma, St Louis, MO) according to the manufacturer's instruction. Total RNA was extracted from 8 individual mouse embryos from 4 different litters at an embryonic day described elsewhere and was mixed before being subjected to labeling. Signals were captured and quantified by use of a GenePix 4000B (Molecular Devices, Sunnyvale, CA).

### ***Evaluation of mitochondrial membrane potential***

A mitochondrion-specific thiol-reactive fluorescent probe (Mito tracker<sup>®</sup> RED CM-H<sub>2</sub>XRos, Invitrogen, Carlsbad, CA) was employed for the evaluation of the mitochondrial membrane potential. *Ccn2*-KO and wild-type chondrocytes were grown to subconfluence in 24-well multiplates and 4-well slide chambers, treated with 200 nM Mito tracker at 37°C for 30 min, washed with PBS, and fixed in 3.7% formaldehyde at 37°C for 15 min. Thereafter, PBS containing 1 µg/ml of 4',6-diamidino-2-phenylindole (DAPI) was added for nuclear staining. Quantitative and qualitative evaluations of mitochondrial activity were conducted by using a high-content analyzing system (Cellomics<sup>™</sup> ArrayScan<sup>®</sup> VTL System, ThermoFisher SCIENTIFIC, Waltham, MA) and an automated microscope (BZ9000, Keyence, Osaka, Japan).

### ***Statistical Analysis***

The results obtained from quantitative experiments were reported as the mean values +/- standard deviation (SD). Statistical comparisons between the groups were performed by using Student's *t*-test. Unless otherwise specified, all experiments were repeated at least twice, and comparable results were obtained.

## **Results**

### ***Depressed biological activities observed in the cartilage of *Ccn2*-null mice***

As found previously (Ivkovic et al., 2003; Kawaki et al., 2008), growth

retardation and delayed chondrocyte differentiation were observed in the *Ccn2*-null mice (Fig. 1A), which findings are in line with our hypothesis that CCN2 may support basic metabolism during cartilage development. First of all, in order to confirm these findings, we comparatively reevaluated the production of cartilaginous ECM *in vivo*, which is the most proper and critical characteristic of chondrocytes. As clearly observed in Fig. 1B, compared with that in the wild type tissue, the content of Alcian blue-stained sulfated proteoglycans was markedly reduced in the developing cartilage from the *Ccn2*-null mice. This result is entirely consistent with previous reports indicating impaired ECM synthesis in the cartilaginous tissues in *Ccn2*-null mice (Ivkovic et al., 2003). Synthesizing proteoglycans is a series of anabolic events that requires energy support. Considering that cell proliferation is also impaired in those cells, these findings collectively suggest depressed energy supply in *Ccn2*-null chondrocytes.

***Metabolic profiles of Ccn2-null chondrocytes that represent a deficiency in basic energy supply system.***

In the living body, a large part of energy is captured through the catabolic pathway, in which acetyl-coenzyme A (CoA) is central. For the comprehensive evaluation of the metabolic outcome of *Ccn2* deletion, metabolome analysis was employed. Absolute quantification of 108 metabolites by CE-TOF MS analysis revealed that the intracellular levels of a number of metabolites were affected by *Ccn2* deletion. Among the catabolic pathways, glycolysis is known as the most fundamental one for energy production, which process is conserved among most organisms. Also, this pathway is regarded as a major catabolic pathway for chondrocytes, since cartilage is an avascular

tissue and thus under hypoxic conditions. Comparative quantification of glycolytic metabolites upstream (Fig. 2A) and downstream (Fig. 2B) of glyceraldehyde 3-phosphate indicated that the intracellular levels of all of the metabolites measured in the *Ccn2*-null chondrocytes were reduced compared with those in the wild-type ones. Particularly, the low level of acetyl-CoA should be noted. The observed overall decrease in the levels of these glycolytic metabolites suggests a fundamental deficiency in the metabolic pathway for biological energy production in the *Ccn2*-null chondrocytes.

***Intractable decrease in the intracellular ATP and other high-energy mononucleotides in *Ccn2*-null chondrocytes***

We repeated the whole quantitative metabolome analysis twice and found remarkable variances in a number of metabolites between 2 experiments. In Fig. 3, the results of 2 independent sets of experiments with independent animals are comparatively plotted. Obviously, a major part of metabolites were reproducibly decreased in the *Ccn2*-null chondrocytes (dots in the blue square); whereas no metabolites with a reproducible increase in these chondrocytes were noted (no dots in the red square). Several metabolites showed quite large variance between the 2 experiments. For example, the hypoxanthine level in *Ccn2*-null chondrocytes was less than that in the wild type in the first evaluation, whereas in the second evaluation, it was more than twice higher in the *Ccn2*-null cells. However, out of 100 metabolites, only 6 of them on the diagonal in Fig. 3 reproducibly yielded a stable reduction in the *Ccn2*-null chondrocytes. Interestingly, ATP was included among these 6 metabolites (the red dot in Fig. 3) and showed the second-largest reduction in *Ccn2*-null cells among

these metabolites. It should be also noted that the intracellular levels of other high-energy mononucleotides, i.e., GTP, CTP, and UTP, were also always decreased by *Ccn2* deletion (Fig. 4A and B). The fact that the relative ratio among the 4 mononucleotides was comparable between *Ccn2*-null and wild-type chondrocytes (Fig. 4A) indicates that the mutual interchange system among these nucleotides was not affected by the *Ccn2* deletion. Considering the stability and strength of the effect of the *Ccn2* deletion on it, together with its having the highest intracellular level among the 4 nucleotides, ATP would supposedly be a critical metabolic target of CCN2 in chondrocytes.

***Recovery of the intracellular ATP level in Ccn2-null chondrocytes by the addition of exogenous CCN2 in vitro***

The results of metabolome analysis via CE-mass spectrometry clearly indicated the requirement of CCN2 for the maintenance of high cellular ATP levels. This finding was further confirmed by a different experimental strategy with a bioluminescence quantification of ATP activity. As exactly indicated by the metabolome analysis, the results of the ATP bioluminescence assay also showed that the ATP level in *Ccn2*-null chondrocytes was decreased by more than 50% in comparison with that in the wild-type ones (Fig. 5A). Utilizing this experimental system, we tested if exogenous CCN2 could rescue the defect in ATP level caused by the *Ccn2* deletion. We added human recombinant CCN2 to cultures of *Ccn2*-null and wild-type chondrocytes and evaluated its effect. This recombinant CCN2 was also used for our very recent study describing the cartilage regenerative effects of CCN2 derivatives and actually showed sufficient biological activities *in vitro* and *in vivo* (Abd El Kader et al., 2013). As expected, the

intracellular ATP level in the *Ccn2*-null chondrocytes was recovered by the treatment with exogenous CCN2 for 48 h (Fig. 5B), whereas it was not significantly by the treatment for 24 h. Of note, the addition of the same amount of CCN2 to the wild-type cultures appeared to increase the ATP level modestly in them as well. Considering that CCN2 enhances cell proliferation and ECM production, both energy-dependent processes, it is reasonable that CCN2 was capable of enhancing ATP synthesis in the chondrocytes.

#### ***Reduction of ATP level in human chondrocytic cells by transient silencing of CCN2***

Since permanent *Ccn2* deletion affects the differentiation of growth plate chondrocytes, cellular compositions along with the differentiation may differ between *Ccn2*-null and wild type growth plates, which may affect metabolic profiles. In order to rule out this possibility, we utilized a human chondrocytic cell line, HCS-2/8, which is widely known to stably retain mature chondrocytic phenotype. By using a synthetic siRNA, CCN2 expression was transiently silenced in HCS-2/8 cells, and cellular ATP level was evaluated. As a result, cellular ATP level was significantly reduced in CCN2-silenced HCS-2/8 cells (Fig. 6). Therefore, ATP reduction in CCN2-depleted chondrocytes is not due to the altered cellular composition, but is caused by individual cellular events.

#### ***Effect of Ccn2 depletion on the expression of various components of the metabolic machinery***

Next, in order to identify genes that mediated the observed phenotypic changes upon *Ccn2* deletion, we performed transcriptome analysis. RNA was extracted and

mixed from 8 individual *Ccn2*-null or wild-type mice from 3 different litters in order to minimize possible individual variation. Microarray analysis of these RNA mixtures showed that the long-term lack of CCN2 increased the expression level of several ribosomal protein genes, i.e., *Rpl38*, *Rpl2*, *Rpl26* and *Rpl35* (Fig. 7A). *Ccn3*, which is another member of the CCN family, was also up-regulated in the *Ccn2*-null chondrocytes, as previously reported (Kawaki et al., 2008). Contrarily, in addition to the genes encoding cartilaginous ECM components, such as type 9 procollagen and aggrecan, a few genes closely related to energy metabolism were repressed by *Ccn2* deletion (Fig. 7B). One such gene was *Atp5l*, encoding the ATP synthase subunit  $\gamma$  in the ATP synthase complex, a critical mitochondrial molecular motor that supplies a major part of cellular ATP through the respiratory chain. In addition, the enolase 1 gene, encoding an enzyme built into the glycolytic pathway, was also found by microarray analysis to have been down-regulated.

#### ***Effect of Ccn2 depletion on mitochondrial activity and Eno1 expression in chondrocytes***

Subsequently, since we found a possible defect in the mitochondrial energy production system through microarray analysis, we next evaluated the biological activity of mitochondria in *Ccn2*-null chondrocytes. Utilizing Mitotracker, which contained a mildly thiol-reactive chloromethyl moiety, we fluorescently labeled only the active mitochondria, in which oxidative phosphorylation occurred. As a result, active mitochondria were efficiently detected in both wild-type and *Ccn2*-null chondrocytes. Although we observed stronger signals in chondrocytes from a few of the wild-type mouse embryos examined (Fig. 8A), quantitative analysis of chondrocytes from several

more animals revealed no significant difference in mitochondrial activity between wild-type and *Ccn2*-null chondrocytes (data not shown). These results suggest a limited involvement of the mitochondria in the observed ATP deficiency in *Ccn2*-null chondrocytes and a relatively minor role of the respiratory chain as a source of ATP in chondrocytes.

Attenuated glycolysis in *Ccn2*-null chondrocytes was also suggested by the data shown in Fig. 2, in which case the involvement of the *Eno1* gene was strongly suspected based on the data in Fig. 7. In order to confirm the repression of the *Eno1* gene in *Ccn2*-null chondrocytes, we performed quantitative real-time RT-PCR analysis and obtained the expected results (Fig. 8B). Therefore, these data strongly suggest that CCN2 regulated ATP production mainly through the anaerobic pathway, specifically targeting the enolase gene.

## **Discussion**

Our present study clearly indicated that the intracellular ATP level was maintained at a higher level in chondrocytes in the presence of CCN2 than in its absence. However, albeit at a reduced rate, even *Ccn2*-null chondrocytes were still capable of proliferating and differentiating even with a drastically reduced intracellular ATP level. Here, we should note that the quantity of ATP we measured does not represent the total quantity that the cell actually produces and consumes. In the cells, ATP is continuously produced and readily used for any anabolic cellular activity. What we could measure was the ATP present in the cells. Interestingly, when we lowered the concentration of



FBS in the medium of *Ccn2*-null chondrocytes to an extremely low one, resulting in cellular dormancy, the quantity of intracellular ATP rose strikingly (data not shown). Thus, even in the absence of CCN2, the chondrocytes were capable of producing the minimal energy to support their basic life functions.

Next, the mechanism by which CCN2 was supporting ATP synthesis was investigated. The results of DNA microarray analysis showed that the lack of CCN2 during development resulted in increased expression of ribosomal protein genes and decreased that of several ECM and metabolism-associated genes. Of note, these genes included the ATP synthase subunit  $\gamma$  gene, the product of which constructs the central shaft of the rotator of the mitochondrial molecular motor (von Ballmoos et al., 2009). The increase in ribosomal protein gene expression could be the outcome of the compensatory survival reaction under energy deficient conditions. Suspecting depressed mitochondrial activity in *Ccn2*-null chondrocytes, we next evaluated the mitochondrial membrane potential. However unexpectedly, no drastic difference in the membrane potential was observed between *Ccn2*-null and wild-type chondrocytes. ATP production through oxidative phosphorylation in mitochondria is the major pathway for cells under normoxic conditions, whereas chondrocytes survive in an avascular microenvironment. Under such an environment, the significance of oxidative phosphorylation for the supply of energy would be expected to be relatively minor, with the anaerobic glycolytic pathway playing the major role in ATP production. In fact in Fig. 2, we showed that the levels of glycolytic metabolites in *Ccn2*-null chondrocytes were overall lower than those in the wild-type ones. Among these metabolites was phosphoenolpyruvate, formed from 2-phosphoglycerate by catalysis by enolase (Wold, 1971). Enolase 1, commonly known as  $\alpha$ -enolase, is the major

isozyme of enolases. Importantly, we found that its expression was significantly decreased in *Ccn2*-null chondrocytes, as determined by quantitative RNA analysis as well as by DNA microarray analysis. We already reported that CCN2 activated extracellular signal-regulated kinase 1/2 in chondrocytes in our previous study (Yosimichi et al., 2006). Importantly, another previous study showed that, through this enolase gene, extracellular signal-regulated kinase 1/2 (ERK1/2) regulates intracellular ATP levels in cardiomyocytes during ischemic hypoxia and reoxygenation (Mizukami et al., 2004). Therefore, CCN2 possibly regulates glycolysis via *Eno1* expression through ERK1/2 signaling pathway in chondrocytes, which is, at least in part, responsible for the observed effects of CCN2 on cellular ATP level. However, the cell surface receptor that initiates this signaling is not defined yet. In addition, since CCN2 interacts a number of other growth factors, indirect effects mediated by such cofactors may not be overlooked. Further investigation to clarify the mechanism of the CCN action in detail is currently ongoing.

ATP is the most important molecule that mediates biological energy transfer for a variety of processes in living organisms. Therefore, a critical basal level of cellular ATP must be present at all times. In contrast, the CCN2 gene is known to be expressed at particular stages during the development of relevant organs (Kubota and Takigawa, 2007). Moreover, *Ccn2* expression is highly restricted to limited tissues in normal adults. These findings again indicate that CCN2 is not indispensable for basic energy metabolism, but is occasionally utilized when an enhanced energy supply is requested. The prominent induction of CCN2 observed upon wound healing is also consistent with this notion. In the growth plate, CCN2 is produced in large quantities only by chondrocytes in the pre-hypertrophic layer (Kubota and Takigawa, 2007, 2011).

After being produced, CCN2 is transported and infiltrates in both directions in the growth plate, forming density gradients (Kawata et al., 2012). On the resting side of the growth plate (upper portion in Fig. 8C), chondrocytes located near the CCN2 producer receive strong CCN2 support that promotes their proliferation, whereas those farther away in the resting layer may not. On the hypertrophic side, ATP production enhanced by a vast number of CCN2 molecule is utilized for early hypertrophic differentiation with vigorous ECM production. CCN2 released in the bone marrow may also promote osteoblasts to proliferate and differentiate (Nishida et al., 2000; Safadi et al., 2003; Smerdel-Ramoya et al., 2008) and vascular endothelial cells to migrate (Shimo et al., 1998 and 1999; Babic et al., 1999) as well (Fig. 8C). Collectively, our results suggest that CCN2 plays an important role in endochondral ossification by enhancing ATP production where it is required.

From a pathogenic point of view, it should be also noted that ATP depletion could be considered as a causative factor for the development of osteoarthritis (OA; Johnson et al., 2004). According to a recent report, impaired ATP production induced by glycolysis inhibitors promotes chondrocyte hypertrophy-like changes leading to the onset and development of OA-like lesions (Nishida et al., 2013). Furthermore, the application of CCN2 to rat OA models induces the regeneration of damaged articular cartilage (Nishida et al., 2004). Considering these findings together with our present results, the anti-OA action of CCN2 may be ascribed to the functional property of CCN2, i.e., prevention of the depletion of ATP. The utility of CCN2 in regenerative medicine for the treatment of cartilaginous tissues is again emphasized herein.

## **Acknowledgements**

The authors have no conflict of interest to declare. Also, the authors thank Drs. Eriko Aoyama and Mitsuhiro Hoshijima for their helpful suggestions, as well as Ms. Yoshiko Miyake for her secretarial assistance.

## **References**

- Abd El Kader T, Kubota S, Nishida T, Hattori T, Aoyama E, Janune D, Hara ES, Ono M, Tabata Y, Kuboki T, Takigawa M. 2013. The regenerative effects of CCN2 independent modules on chondrocytes in vitro and osteoarthritis models in vivo. Bone in press.
- Babic AM, Chen CC, Lau LF. 1999. Fisp12/mouse connective tissue growth factor mediates endothelial cell adhesion and migration through integrin alphavbeta3, promotes endothelial cell survival, and induces angiogenesis in vivo. *Mol Cell Biol* 19: 2958-2966.
- Brigstock DR, Goldschmeding R, Katsube K, LamSCT, Lau LF, Lyons K, Naus C, Perbal B, Riser B, Takigawa M, Yeger H. 2003. Proposal for a unified CCN nomenclature. *Mol Pathol* 56: 127-128.
- Hattori T, Müller C, Gebhard S, Bauer E, Pausch F, Schlund B, Bösl MR, Hess A, Surmann-Schmitt C, von der Mark H, de Crombrughe B, von der Mark K. 2010. SOX9 is a major negative regulator of cartilage vascularization, bone marrow formation and endochondral ossification. *Development* 137: 901-911.
- Ivkovic S, Yoon BS, Popoff SN, Safadi FF, Libuda DE, Stephenson RC, Daluiski A, Lyons KM. 2003. Connective tissue growth factor coordinates chondrogenesis and

- angiogenesis during skeletal development. *Development* 130: 2779-2791.
- Johnson K, Svensson CI, Etten DV, Ghosh SS, Murphy AN, Powell HC, Terkeltaub R. 2004. Mediation of spontaneous knee osteoarthritis by progressive chondrocyte ATP depletion in Hartley guinea pigs. *Arthritis Rheum* 50:1216-1225
- Jun JI, Lau LF. 2011. Taking aim at the extracellular matrix: CCN proteins as emerging therapeutic targets. *Nat Rev Drug Discov* 10: 9459-9463.
- Kawaki H, Kubota S, Suzuki A, Lazar N, Yamada T, Matsumura T, Ohgawara T, Maeda T, Perbal B, Lyons KM, Takigawa M. 2008. Cooperative regulation of chondrocyte differentiation by CCN2 and CCN3 shown by a comprehensive analysis of the CCN family proteins in cartilage. *J Bone Miner Res* 23: 1751-1764.
- Kawata K, Kubota S, Eguchi T, Aoyama E, Moritani NH, Kondo S, Nishida T, Takigawa M. 2012. Role of LRP1 in transport of CCN2 protein in chondrocytes. *J Cell Sci* 125: 2965-2972.
- Kubota S, Takigawa M. 2007. Role of CCN2/CTGF/Hcs24 in bone growth. *Int Rev Cytol* 257: 1-41.
- Kubota S, Takigawa M. 2011. The role of CCN2 in cartilage and bone development. *J Cell Commun Signal* 8: 209-217.
- Kubota S, Takigawa M. 2007. CCN family proteins and angiogenesis: from embryo to adulthood. *Angiogenesis* 10: 1-11.
- Leask A, Abraham DJ. 2006. All in the CCN family: essential matricellular signaling modulators emerge from the bunker. *J Cell Sci* 119: 4803-4810.
- Mizukami Y, Iwamatsu A, Aki T, Kimura M, Nakamura K, Nao T, Okusa T, Matsuzaki M, Yoshida K and Kobayashi S. 2004. ERK1/2 regulates intracellular ATP levels through a-enolase expression in cardiomyocytes exposed to ischemic hypoxia and

reoxygenation. *J Biol Chem* 279: 50120-50131.

Nakanishi T, Kimura Y, Tamura T, Ichikawa H, Yamaai Y, Yugimoto T and Takigawa M. 1997. Cloning of an mRNA preferentially expressed in chondrocytes by differential display-PCR from a human chondrocytic cell line that is identical with connective tissue growth factor (CTGF) mRNA. *Biochem Biophys Res Commun* 234: 206-210.

Nakanishi T, Nishida T, Shimo T, Kobayashi K, Kubo T, Tamatani T, Tezuka K and Takigawa M. 2000. Effects of CTGF/Hcs24, a product of a hypertrophic chondrocyte-specific gene, on the proliferation and differentiation of chondrocytes in culture. *Endocrinology* 141: 264-273.

Nishida T, Nakanishi T, Asano M, Shimo T, Takigawa M. 2000. Effects of CTGF/Hcs24, a hypertrophic chondrocyte-specific gene product, on the proliferation and differentiation of osteoblastic cell in vitro. *J Cell Physiol* 184: 197-206.

Nishida T, Kubota S, Nakanishi T, Kuboki T, Yoshimichi G, Kondo S, Takigawa M. 2002. CTGF/Hcs24, a hypertrophic chondrocyte-specific gene product, stimulates proliferation and differentiation, but not hypertrophy of cultured articular chondrocytes. *J Cell Physiol* 192: 55-63.

Nishida T, Kubota S, Kojima S, Kuboki T, Nakao K, Kushibiki T, Tabata Y, Takigawa M. 2004. Regeneration of defects in articular cartilage in rat knee joints by CCN2 (connective tissue growth factor). *Bone Miner Res* 19: 1308-1319.

Nishida T, Kubota S, Aoyama E, Takigawa M. 2013. Impaired glycolytic metabolism causes chondrocyte hypertrophy-like changes via promotion of phosphor-Smad 1/5/8 translocation into nucleus. *Osteoarthritis and Cartilage*. 21: 700-709.

Perbal B. 2004. CCN proteins: multifunctional signaling regulators. *Lancet*. 363:62-64

- Perbal B, Takigawa M. 2005. CCN protein -A new family of cell growth and differentiation regulators-, London: Imperial College Press. 311p.
- Safadi FF, Xu J, Smock SL, Kanaan RA, Selim AH, Odgren PR, Marks SC Jr, Owen TA, Popoff SN. 2003. Expression of connective tissue growth factor in bone: its role in osteoblast proliferation and differentiation *in vitro* and bone formation *in vivo*. *J Cell Physiol* 196: 51-62.
- Shimo T, Nakanishi T, Kimura Y, Nishida T, Ishizeki K, Matsumura T, Takigawa M. 1998. Inhibition of endogenous expression of connective tissue growth factor by its antisense oligonucleotide and antisense RNA suppresses proliferation and migration of vascular endothelial cells. *J Biochem* 124: 130-140.
- Shimo T, Nakanishi T, Nishida T, Asano M, Kanyama M, Kuboki T, Tamatani T, Tezuka K, Takemura M, Matsumura T, Takigawa M. 1999. Connective tissue growth factor induces the proliferation, migration, and tube formation of vascular endothelial cells *in vitro*, and angiogenesis *in vivo*. *J Biochem* 126: 137-145.
- Smerdel-Ramoya A, Zanotti S, Deregowski V, Canalis E. 2008. Connective tissue growth factor enhances osteoblastogenesis *in vitro*. *J Biol Chem* 283: 22690-22699.
- Takigawa M. 2013. CCN2: a master regulator of the genesis of bone and cartilage. *J Cell Commun Signal* 7: 191-201.
- Takigawa M, Takano T, Suzuki F. 1981. Effects of parathyroid hormone and cyclic AMP analogues on the activity of ornithine decarboxylase and expression of the differentiated phenotype of chondrocytes in culture. *J Cell Physiol* 106: 259-268
- Takigawa M, Nakanishi T, Kubota S, Nishida T. 2003. Role of CTGF/HCS24/ecogenin in skeletal growth control. *J Cell Physiol*. 194: 256-266.
- von Ballmoos C, Wiedenmann A, Dimroth P. 2009. Essentials for ATP synthesis by

F1F0 ATP synthases. *Annu Rev Biochem* 78:649-672.

Wold F. 1971. Enolase, in *The Enzymes*. (Boyer, P.D.,ed) Academic Press, New York. 499-538.

Weksler NB, Lunstrum GP, Reid ES and Horton WA. 1999. Differential effects of fibroblast growth factor (FGF) 9 and FGF2 on proliferation, differentiation and terminal differentiation of chondrocytic cells in vitro. *Biochem J* 342: 677-682.

Yosimichi G, Kubota S, Nishida T, Kondo S, Yanagita T, Nakao K, Takano-Yamamoto T, Takigawa M. 2006. Roles of PKC, PI3K and JNK in multiple transduction of CCN2/CTGF signals in chondrocytes. *Bone* 38: 853-863.



## Figure Legends

**Fig. 1.** The phenotype in growth-plate cartilage of *Ccn2*-null mice, representing metabolic depression. **A.** Overview of phenotypic changes caused by *Ccn2* deletion. Findings observed in our previous study by Kawaki et al. are summarized. *Ccn2* deletion caused a remarkable reduction in chondrocyte proliferation and extracellular matrix (ECM) synthesis and maturation *in vivo* and *in vitro*, which was accompanied by decreased expression of chondrocytic marker genes. Note that *Ccn3* expression was enhanced by *Ccn2* deletion. **B.** Impaired proteoglycan synthesis in the growth plate revealed by Alcian blue staining. Representative views at low power (upper panels) and high power (lower panels) magnifications are shown. The reduced staining in the growth plate of this *Ccn2*-null mouse is consistent with the phenotype summarized in panel A. Scale bars: 200  $\mu\text{m}$  (upper panels); 100  $\mu\text{m}$  (lower panels).

**Fig. 2.** Effects of *Ccn2* deletion on the metabolites involved in glycolysis. Glycolytic metabolites upstream (A) and downstream (B) of glyceraldehyde 3-phosphate in each type of chondrocyte were quantified. The vertical axis of the graph represents metabolite content in  $10^6$  chondrocytes ( $\text{pmol}/10^6\text{cells}$ ). Open and solid columns represent the data from the wild-type and *Ccn2*-null chondrocytes, respectively. The entire experiments were repeated twice, which always indicated lower levels of these metabolites in *Ccn2*-null mice (KO) than in the wild-type (WT) ones. The mean values of 2 sets of the experiments are shown with error bars of standard deviations, except for fructose 6-phosphate that was not detectable in one of the experiments.

**Fig. 3.** Comparative analysis of the data obtained by 2 sets of metabolome analysis. Relative metabolite levels in *Ccn2*-null chondrocytes versus those in wild-type chondrocytes were computed for the metabolites that were successfully quantified in both sets of experiments. The data from the first (ordinate) and second (abscissa) evaluations are plotted on the single graph. Constant elevation of or reduction in levels of metabolites is indicated by the dots in the square areas shown in red or blue, respectively. Note the absence of dots in the red square, whereas most of the dots are in the blue area, representing fundamental metabolic depression. Dots on the dotted diagonal line represent the relative changes in metabolite levels that were exactly stable between 2 independent sets of experiments. The red dot denotes the data for ATP; and the yellow ones, those for GTP, CTP and UTP.

**Fig. 4.** Absolute quantification of high-energy mononucleotides in *Ccn2*-null and wild-type chondrocytes. The mean values of the metabolite contents from independent metabolome analyses are shown with standard deviations. **A.** Comparison among the mononucleotides in each type of chondrocyte. Upper: Quantifications of ATP, CTP, GTP, and UTP in wild-type (WT) chondrocytes. Lower: Quantifications of ATP, CTP, GTP and UTP in *Ccn2*-null chondrocytes. The normal ratio among the mononucleotide contents observed in the wild type is retained in the *Ccn2*-null chondrocytes, with the highest level being that of ATP. **B.** Comparison of nucleotide levels between the wild-type and *Ccn2*-null (KO) chondrocytes. The levels of these high-energy mononucleotide in *Ccn2*-null chondrocytes (KO) were stably lower than those in the WT ones by approximately 50%. The ordinate indicates the absolute content of each

mononucleotide (pmol/10<sup>6</sup>cells).

**Fig. 5.** Effect of CCN2 on the intracellular ATP levels measured by a bioluminescence assay. **A.** Comparison between *Ccn2*-null and wild-type chondrocytes. Chondrocytes were isolated from mice and cultured in 6-well multi-well plates as primary cultures. After the cells had reached confluence, they were recollected and inoculated at a density of  $2 \times 10^5$ /plate into 24-well multi-well plates. After 3 days, ATP quantification was performed as described in Materials and Methods. By use of a BCA Protein Assay kit (Thermo Fisher Scientific), quantification of total proteins was also conducted to standardize the data. The intracellular ATP levels are presented as relative amounts of ATP per total cellular protein. Evaluation was performed in triplicate. \* $p < 0.05$ , significantly different from wild type (WT) control. **B.** Effect of exogenous CCN2 on the intracellular ATP levels. The cells were prepared as described for panel A, incubated for 48 h in DMEM medium containing 50 ng/ml rCCN2/DMEM and 10% FBS, and then analyzed for their ATP level. ATP levels are represented as relative values against those in KO cells without rCCN2 treatment. Data are means  $\pm$ SD of relative values from each cell culture against the WT (-) control.

**Fig. 6.** Effect of transient silencing of *CCN2* on cellular ATP level in human chondrocytic HCS-2/8 cells. **A.** Silencing of *CCN2* by an siRNA. HCS-2/8 cells were transfected with synthetic siRNA against *CCN2* (siCCN2) or control (NC) RNA, and *CCN2* mRNA was quantified 48 h later. **B.** Quantification of cellular ATP under the same conditions as those for panel A. Experiments were performed in

quadruplicate, and means  $\pm$ SD are shown. \* $p < 0.05$  and \*\* $p < 0.01$ , significantly different from NC.

**Fig. 7.** Effect of *Ccn2* deletion on the expression of metabolism-associated genes in chondrocytes. **A.** Genes up-regulated by *Ccn2* deletion, as revealed by DNA microarray analysis. *Rpl38*, *Rpl2*, *Rpl26*, and *Rpl35* indicate the genes for ribosomal proteins L38, L2, L26, and L35, respectively. *Ccn3* is another CCN family member that was earlier reported to be up-regulated in CCN2-deficient mice. **B.** Genes down-regulated by *Ccn2* deletion, as revealed by DNA microarray analysis. *Eno1*, *Col9A1*, *Atp51*, and *Acan* represent enolase 1, type 9 procollagen alpha 1 chain, ATP synthase subunit  $\gamma$  and aggrecan genes, respectively. Note that the expression of 2 of these energy metabolism-associated genes (Eno1 and Acan), as well as that of ECM component-encoding ones, was reduced by *Ccn2* deletion.

**Fig. 8.** Contribution of mitochondrial and glycolytic factors to the ATP deficiency in *Ccn2*-null chondrocytes. **A.** Fluorescence staining of active mitochondria with membrane potential by Mitotracker. Signals in wild-type (WT) chondrocytes appeared to be slightly stronger than those in *Ccn2*-null ones, but no statistically significant difference was observed between the two (data not shown). **B.** Reduced gene expression of enolase 1, which is one of the major glycolytic enzymes, in *Ccn2*-null chondrocytes. Data were obtained by real-time RT-PCR of the RNAs from the littermates, suggesting impaired glycolysis therein. Evaluation was performed in triplicate. \*\* $p < 0.01$ , significantly different from the WT control. **C.** Role of CCN2 as a metabolic supporter in the growth plate. The growth plate is schematically

represented along with an illustration of a long bone. RC, resting chondrocyte; PC, proliferating chondrocyte; PHC, pre-hypertrophic chondrocyte; HC, hypertrophic chondrocyte; VE, vascular endothelial cell, Ob, osteoblast. Stars with "C" denote CCN2 molecules. In the process of endochondral ossification, CCN2 is mostly produced by pre-hypertrophic chondrocytes. CCN2 stimulates the energy production to promote the proliferation of the proliferating chondrocytes on the upper side. On the lower side, hypertrophic differentiation accompanied by the production of ECM molecules and matrix vesicles is promoted under the metabolic support by CCN2. The schema also indicates that CCN2 may enhance the activity and migration of osteoblasts and vascular endothelial cells.

**A**

| <b>Biological Activity</b> |   | <b>Gene expression</b> |   |
|----------------------------|---|------------------------|---|
| Cell proliferation         | ↓ | <i>Sox 9</i>           | ↓ |
| Proteoglycan synthesis     | ↓ | <i>Acan</i>            | ↓ |
| Matrix calcification       | ↓ | <i>Col II a (1)</i>    | ↓ |
|                            |   | <i>Ccn3</i>            | ↑ |

**B**

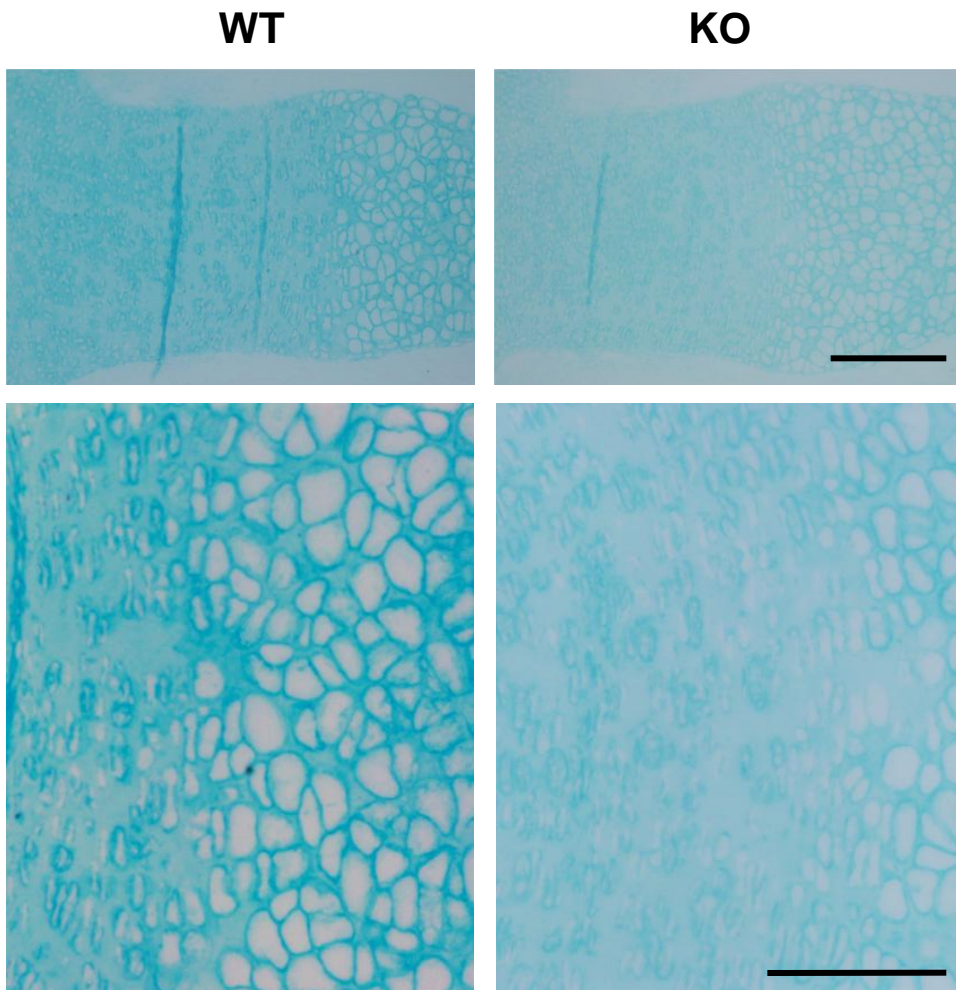
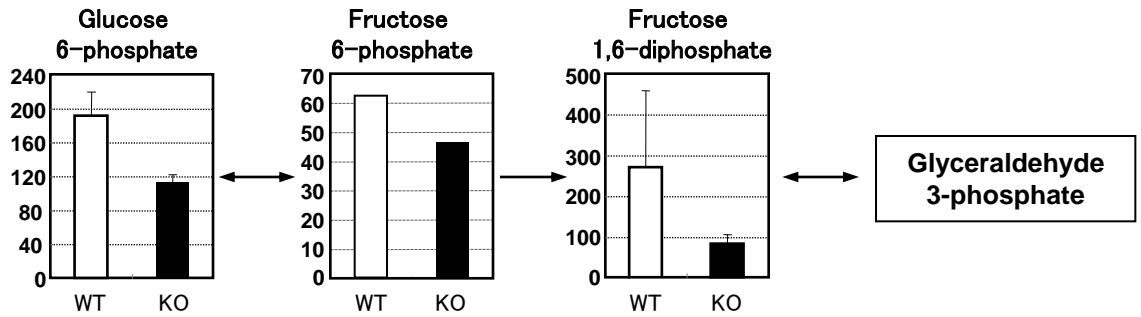


**Fig. 1. Maeda et al.**

**A**



**B**

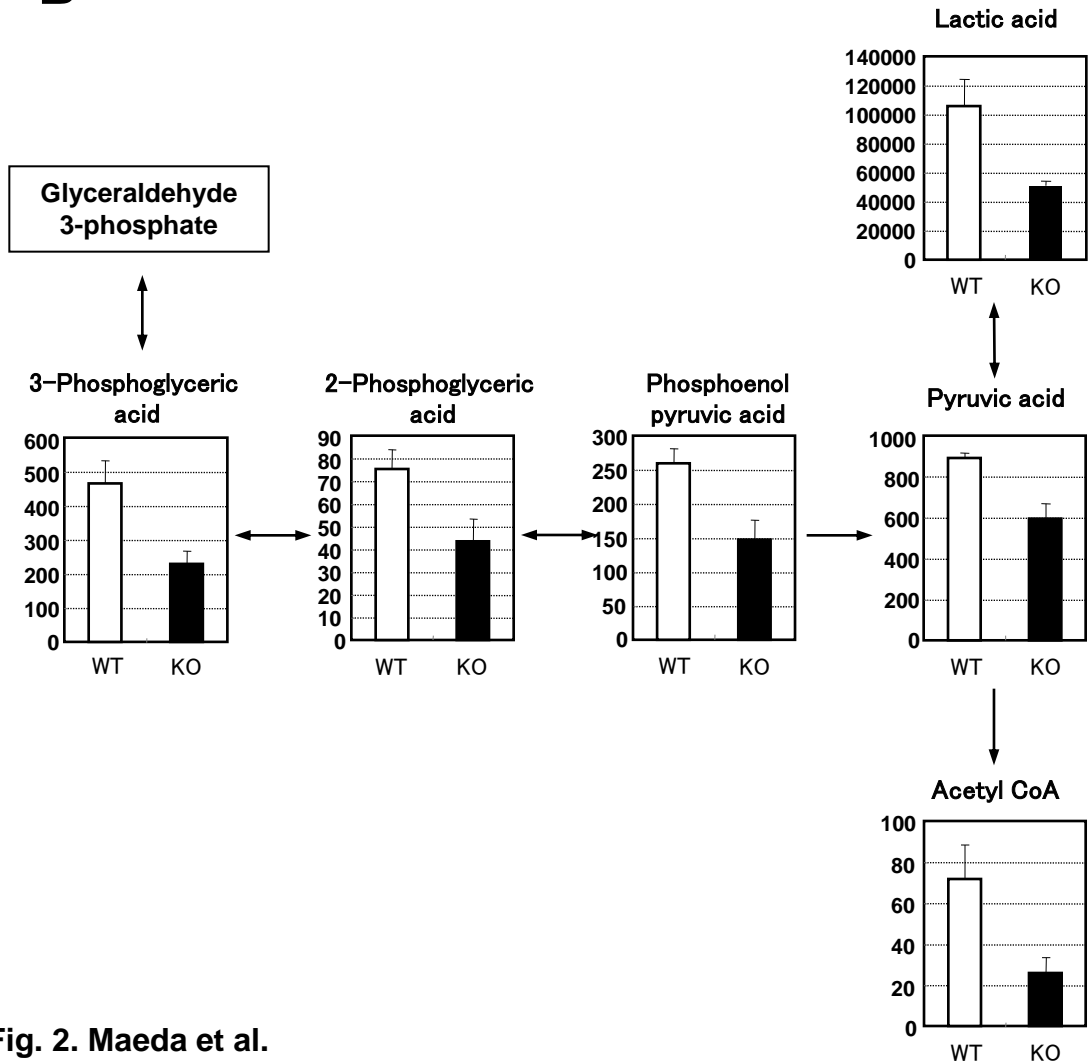


Fig. 2. Maeda et al.

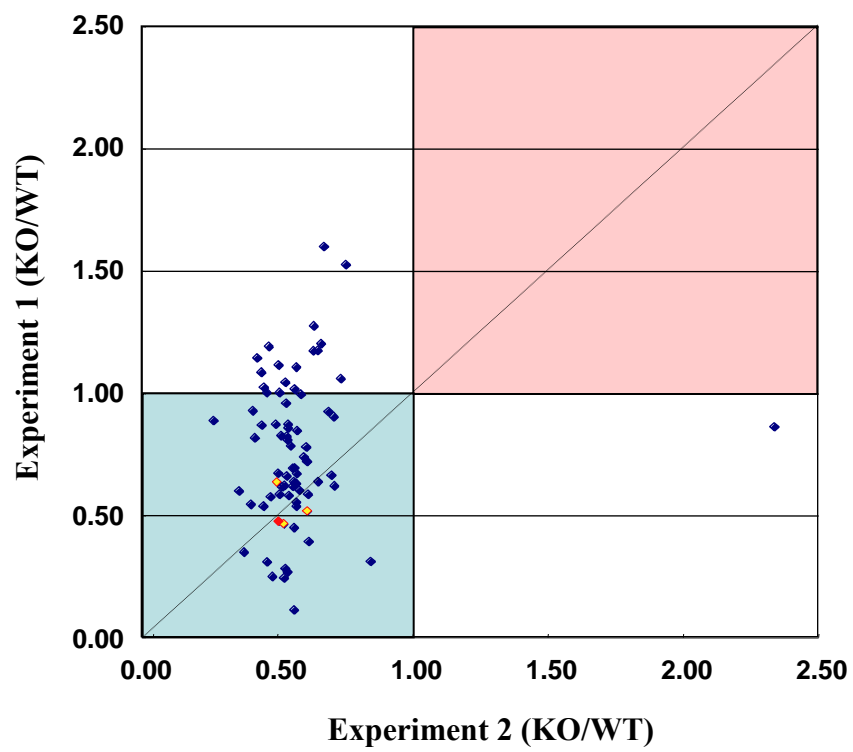


Fig. 3. Maeda et al.



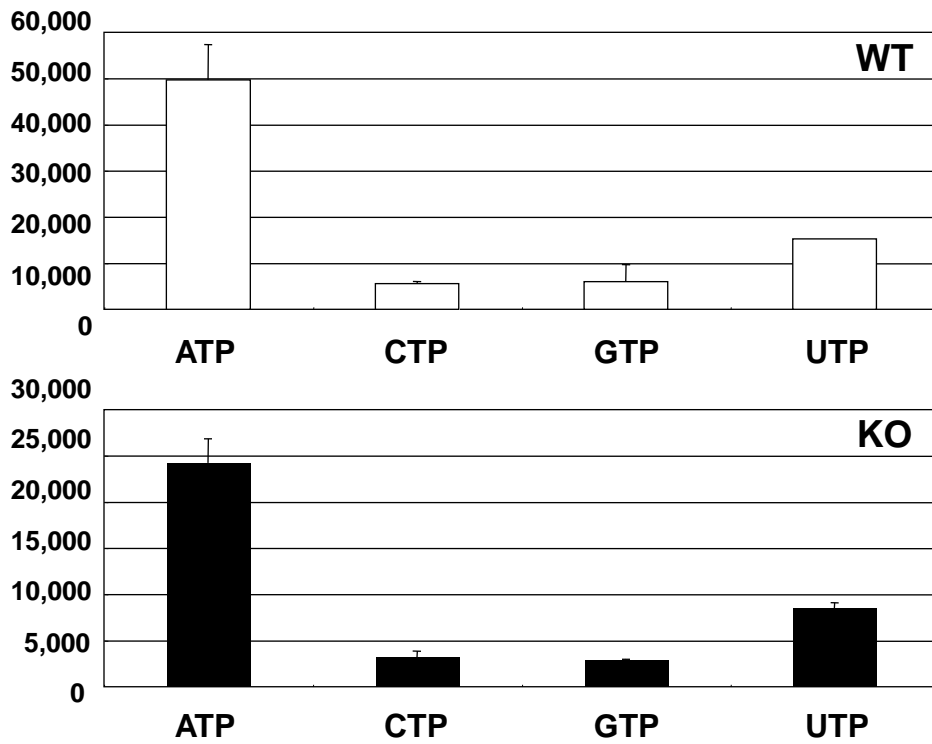
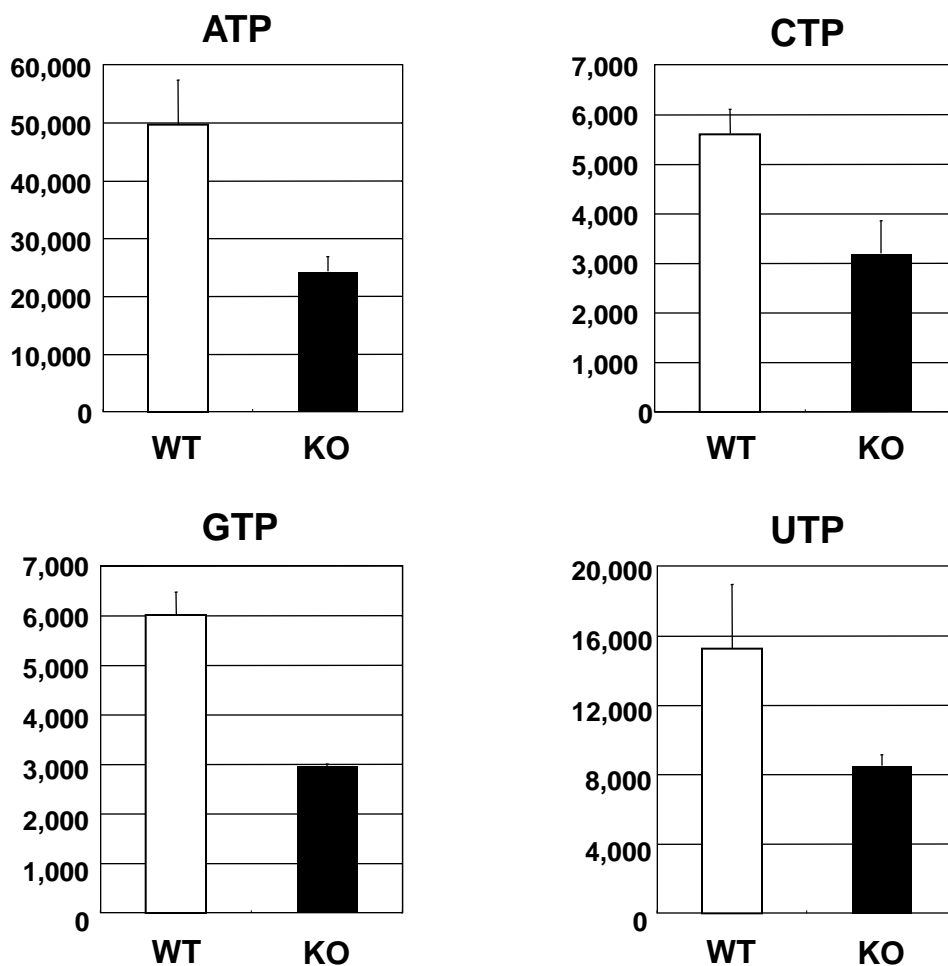
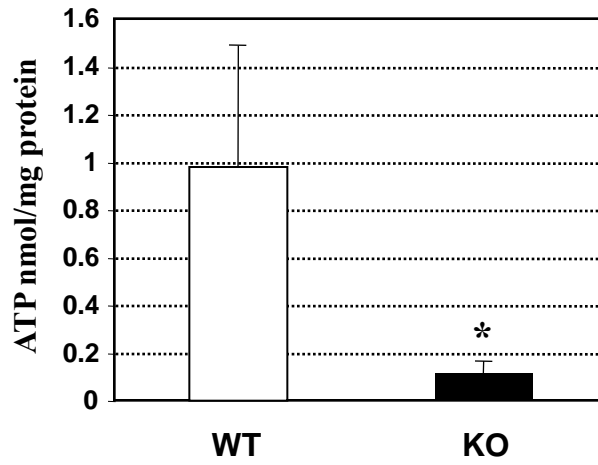
**A****B**

Fig. 4. Maeda et al.

**A**



**B**

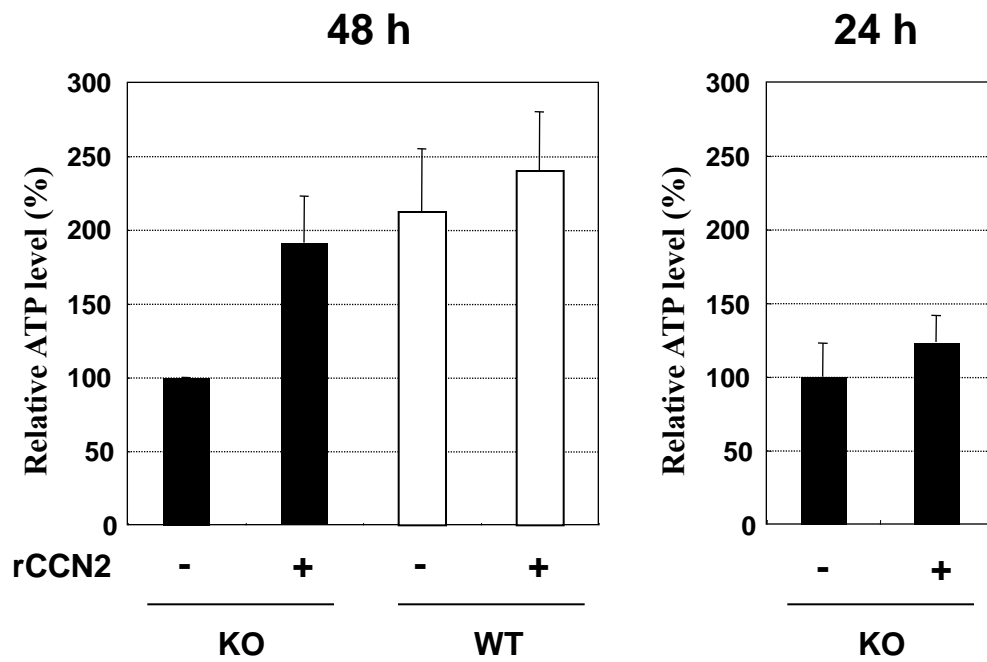
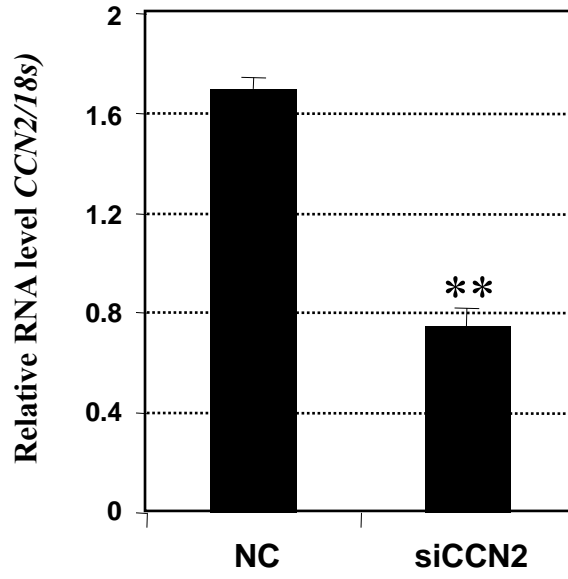


Fig. 5. Maeda et al.

**A**



**B**

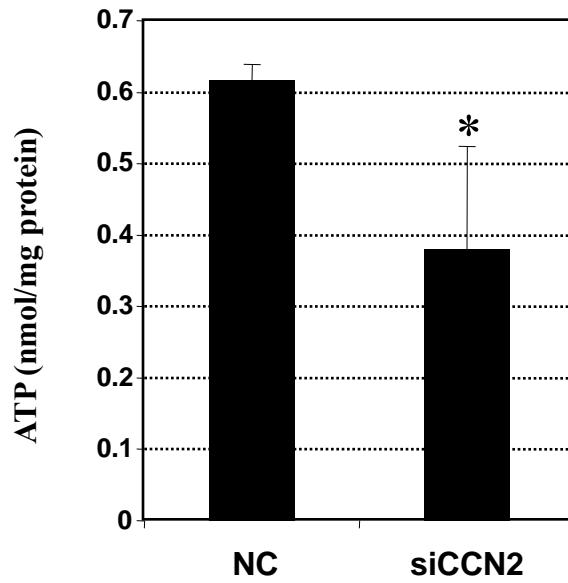


Fig. 6. Maeda et al.

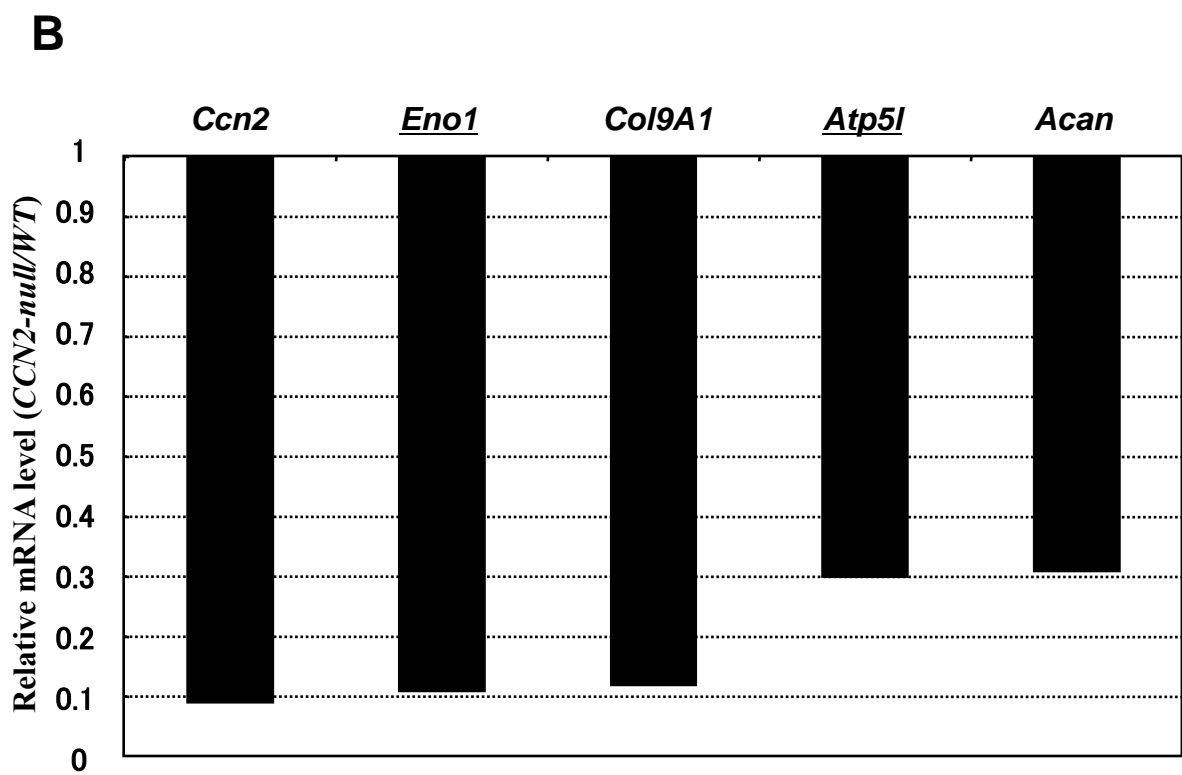
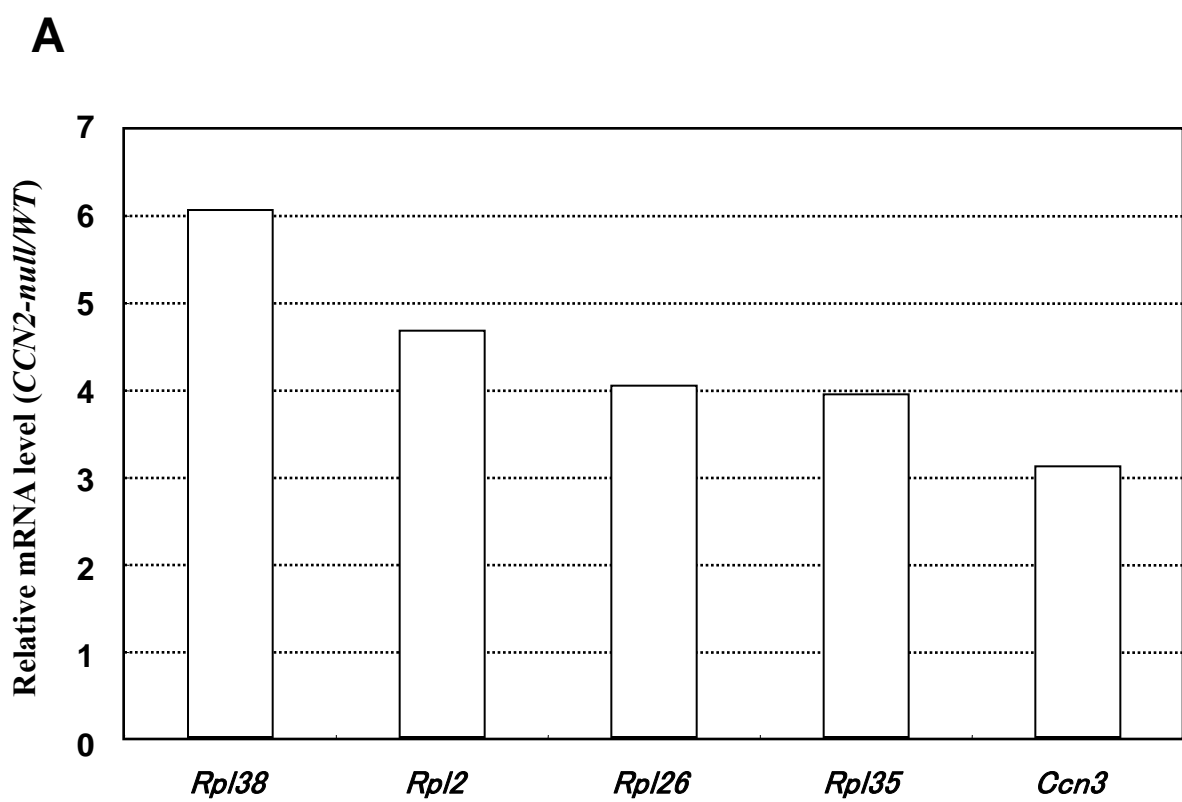
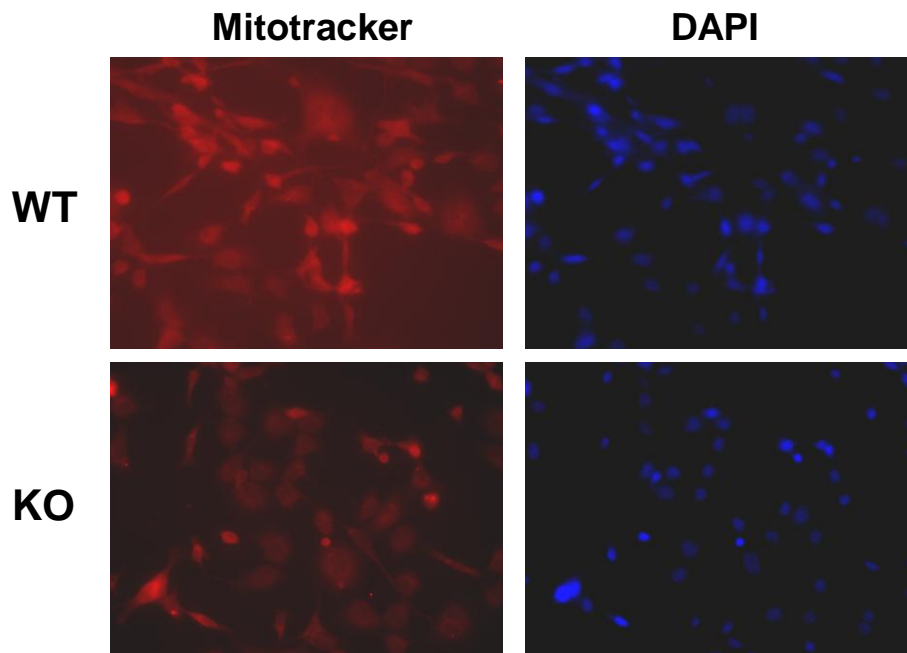
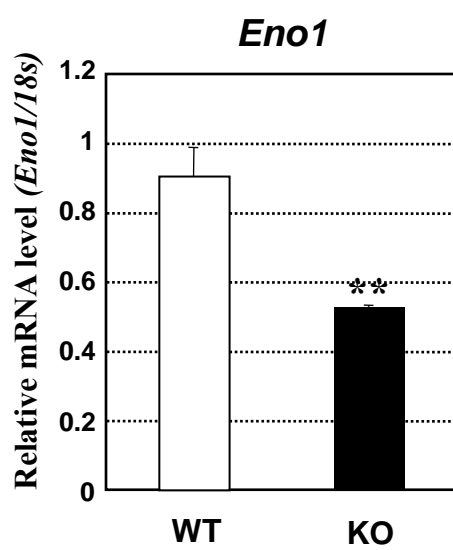
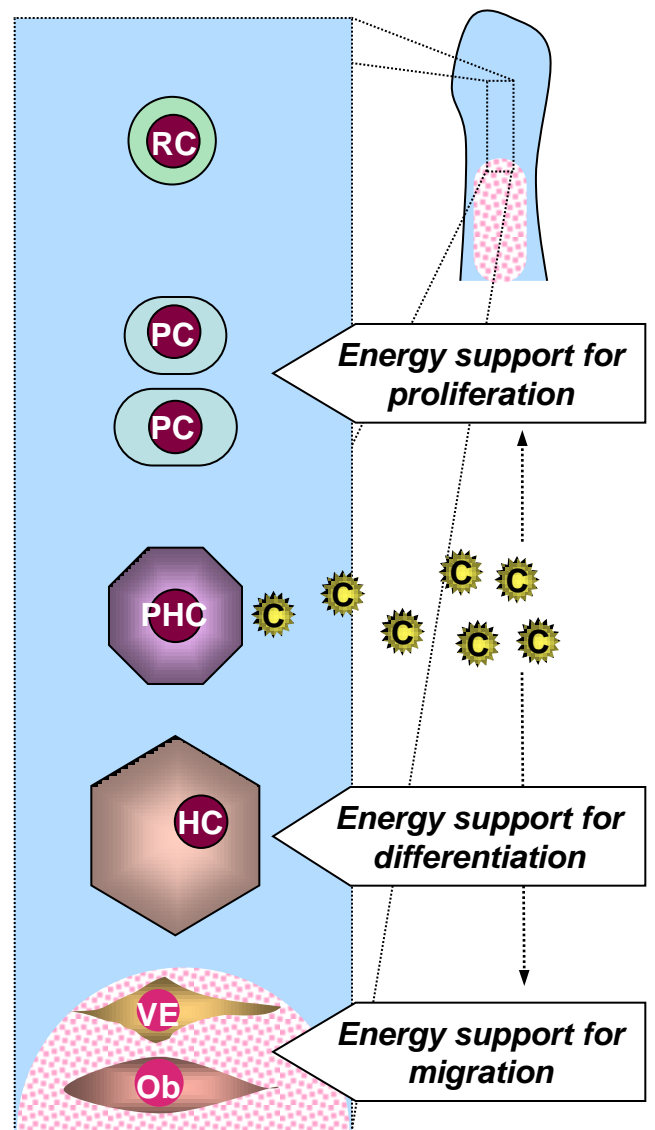


Fig. 7. Maeda et al.

**A****B****C**

**Fig. 9.** Maeda et al.